3P4-11

Proceedings of Symposium on Ultrasonic Electronics, Vol. 37 (2016)
16-18 November, 2016

Study of rectangular vibrating plate size of aerial ultrasonic source combined with rigid wall
矩形たわみ振動板と剛壁が一体構造の空中超音波音源における振動板の大きさの検討

Ryo Sato‡, Takuya Asami, Hikaru Miura (Coll.of Sci. & Tech.,Nihon Univ.)
佐藤　諒‡，淺見拓哉，三浦　光（日大・理工）

1. Introduction

Ultrasonic sound sources can radiate strong ultrasonic into the air by using a stripe mode rectangular vibrating plate or a lattice mode square vibrating plate. These sound sources are used in various fields such as deodorization and aerosol aggregation. For those applications, a vibrating plate and several reflective plates are used to form a standing wave field. However, the reflective plates cannot be fixed to the vibrating plate and a gap is formed between parts. Therefore, we have combined the sound source with rectangular vibrating plate and rigid walls to solve those problems. Rigid walls are integrated into the parallel side in the direction of the nodal line of the stripe mode of the rectangular vibrating plate. Therefore, this sound source has the advantages of easily forming a closed area, the rigid wall being fixed to the other parts, and the configuration being simple. We previously reported that a standing wave field is formed in the enclosure by the vibrating plate, rigid walls and a parallel refractive plate. [1)] In this report, we investigate the size of the vibrating plate and the relationship between input power and sound pressure to determine the conditions for driving the stripe mode at the resonance frequency.

2. Aerial ultrasonic sound source

Figure 1 shows a schematic diagram of the ultrasonic source with a vibrating plate. The sound source consists of a 20 kHz bolt-clamped Langevin transducer, an exponential horn, a resonance rod, and a vibrating plate combined with rigid walls. In this design, the both ends of the stripe mode rectangular vibrating plate is the fixed end and driving point is in the center. The interval between the nodal lines of the stripe mode vibrating plate, *d,* is related to the vertical plate end length in the direction of the nodal lines, *L*, and the plate length parallel to the nodal lines, *W,* by

$$d = \sqrt{\frac{\pi C_D h}{2f}} \tag{1}$$

$$L = (N_L - 0.5)d \tag{2}$$

$$W = N_W d \tag{3}$$

where, C_d is a material constant, h is the plate thickness, f is the resonance frequency, N_L is an even number and N_W is an odd number. **Figure 2** shows a schematic diagram of the vibrating plate where N_L is 12,

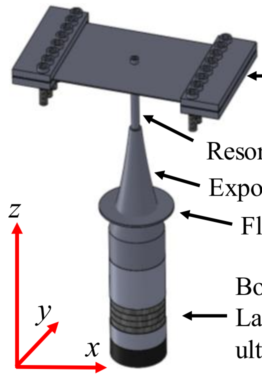

Fig. 1. Schematic of the ultrasonic source.

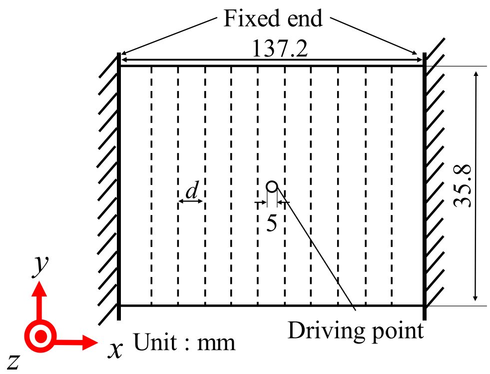

Fig. 2. Schematic of the vibrating plate (N_W=9).

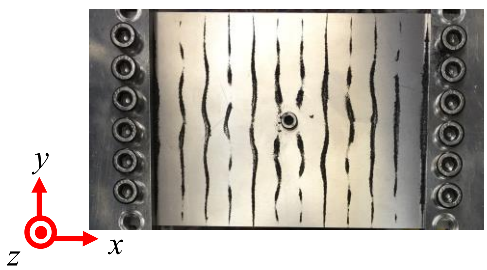

Fig. 3. Chladni figure of a vibrating plate with two fixing tools (N_W=9).

E-mail : csry15016@g.nihon-u.ac.jp‡
asami.takuya@nihon-u.ac.jp
miura.hikaru@nihon-u.ac.jp

N_W is 9, d is 11.9 mm, and the nodal lines are shown as dashed lines. The vibrating plate consists of 1.2-mm-thick duralumin (A2017), and the stripe-mode resonance frequency of this sound source is 20.0 kHz. We use fixing tools to restrain the vibrating end of the vibrating plate in the ultrasonic source with rigid walls.

3. Study of rectangular vibrating plate size

To investigate the size of the rectangular vibrating plate, we investigate the effect of varying W on N_W. We measure whether the stripe mode at resonance is formed for N_L of 12 and N_W of 3, 5, 7, or 9. **Table 1** shows that in each case, the stripe mode is formed at resonance. **Figure 3** shows the Chladni figure of a vibrating plate for N_W of 9. Fixing tools are set at both ends of the plate, and the black lines are sand showing the nodal lines of vibration. Therefore, N_W fits an odd number.

4. Sound pressure distribution of the aerial standing wave field

To determine the sound pressure distribution of the standing wave field formed by the vibrating plate, rigid walls, and a parallel refractive plate, we investigate the distribution of sound pressure. The input power is set to a constant 0.5 W, and the resonance frequency is set to a constant 20.0 kHz. The parallel refractive plate is located 75.8 mm from the vibrating plate. The sound pressure is measured in the x-z plane on a quarter of a narrow side length (red one point broken line in Fig. 2) using a microphone on a probe (TYPE-7017, ACO) with N_L of 12 and N_W of 9. **Figure 4** shows the sound pressure distribution in the x-z plane. The sound pressure is normalized to the maximum value of the microphone output voltage and is shown by color scale. An aerial standing wave field is formed toward the x and z-axes, and the intervals of the sound pressure antinodes are approximately 12 mm.

5. Sound pressure of an antinode of standing wave field

To determine the relationship between input power and sound pressure of an antinode in the standing wave field, we investigate the sound pressure using 1/8 in. microphone (TYPE-7118, ACO). Measurements are conducted at the points of the highest sound pressure in Fig. 4. **Figure 5** shows the sound pressure as a function of input power. The horizontal axis represents the input power and the vertical axis represents the sound pressure. The sound pressure is approximately proportional to the square root of the input power. The sound pressure at an input power of 30 W is 2.97 kPa (sound pressure level of 163 dB).

6. Conclusions

We investigated the parallel plate end length in the direction of the nodal lines and the relationship between the input power and sound pressure in the sound source with a rectangular vibrating plate and rigid walls. Our results show that N_W fits to an odd number and the sound pressure of the antinodes of the standing wave field increase with increasing input power.

Acknowledgment

Part of this work was supported by JSPS KAKENHI Grant Number 15K05875.

References

1. R.Sato, T.Asami and H.Miura : *Proc. National Spring Meet Acoust. Soc.Jpn.* (2016) pp.1139-1140 [in Japanese]

Table 1. Occurrence of stripe mode at resonance. ○: stripe mode at roccurs at the resonance frequency.

N_L	N_W			
	3	5	7	9
12	○	○	○	○

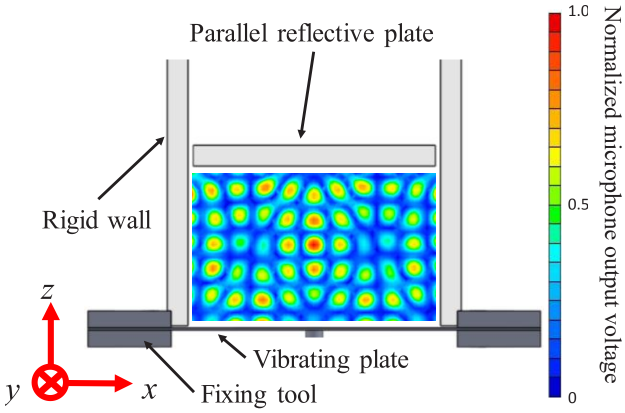

Fig. 4. Sound pressure distribution in the x-z plane with a parallel reflective plate.

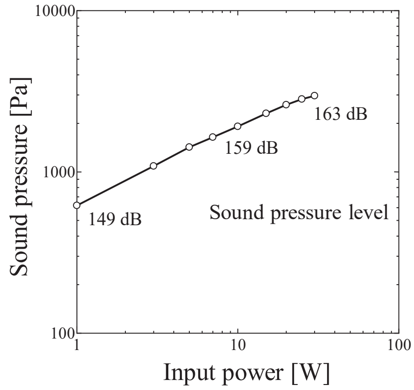

Fig. 5. Relationship between input power and sound pressure.